IOP Conf. Series: Materials Science and Engineering **320** (2018) 012006 doi:10.1088/1757-899X/320/1/012006

A Two-stage Improvement Method for Robot Based 3D Surface Scanning

F B He[1], Y D Liang[1,2], R F Wang[1] and Y S Lin[3]
[1] School of Mechanical Engineering, Dalian University of Technology, Dalian 116024, China
[2] Engineering Training Center, Dalian University of Technology, Dalian 116024, China
[3] Department of Computer Science, Dalian Ocean University, Dalian 116023, China

E-mail: hefuben@mail.dlut.edu.cn

Abstract. As known that the surface of unknown object was difficult to measure or recognize precisely, hence the 3D laser scanning technology was introduced and used properly in surface reconstruction. Usually, the surface scanning speed was slower and the scanning quality would be better, while the speed was faster and the quality would be worse. In this case, the paper presented a new two-stage scanning method in order to pursuit the quality of surface scanning in a faster speed. The first stage was rough scanning to get general point cloud data of object's surface, and then the second stage was specific scanning to repair missing regions which were determined by chord length discrete method. Meanwhile, a system containing a robotic manipulator and a handy scanner was also developed to implement the two-stage scanning method, and relevant paths were planned according to minimum enclosing ball and regional coverage theories.

1. Introduction

Aiming at measuring and recognizing the topography and contour of unknown object, the laser scanning was applied to collect 3D data as much as possible trying to reconstruct the surface. As a non-contact measurement technology, it owned many advantages, which had been widely applied in various engineering fields. To perform automatic 3D laser scanning application, recent studies mainly adopted the method of prediction estimation to plan the sampling points, the viewpoints and the scanning paths so as to obtain the complete 3D information of the surface. For example, to apply a mass vector chain to determine the exploration direction and the accurate position in the viewpoint planning of 3D model reconstruction [1], to present a next-best-scan (NBS) approach to plan collision free path in order to completely scan unknown objects [2], an adaptive sampling method presented to plan the measuring path according to the curvature feature of the fitted B-splines [3], using a model-based viewpoint planning method to inspect freeform surface [4], and a new next-best-view (NBV) planning method proposed for reconstruction of unknown 3D model based on limit visual surface [10], etc. However, the missing region determine errors, the sampling point arrangement errors, the viewpoint deviations and other problems still existed in unknown surface scanning in spite of these studies had been demonstrated in some experimental applications. Furthermore, some of scanning methods might consume amount of resources by algorithm operations in the process and the speed was quite slow in pursuit of the completeness of scanning. To improve the quality of 3D scanning with consideration of speed, the paper presented a two-stage scanning method including the firstly rough scanning and secondly specific scanning. The idea was to scan the object in a faster speed so as to obtain general 3D information of surface, which would reduce scanning time immensely, then to

analyse and to determine whether the collected data existed missing regions. If the missing regions were confirmed, one more detailed scanning seemed to be very necessary to complete the scanning process. In the laser 3D scanning, point cloud data was collected from the surface and was able to be converted to spatial data points. Then it needed to apply mathematics algorithms to confirm the locations and orientation of the missing regions. In the scanning path planning, the minimum enclosing ball (MEB) theory [5-8] was introduced, since MEB had been already applied in solving large data sets problem [5,8] and evaluating the barycentre error in large blade optimization process [6,7]. It represented a ball field with the minimum radius to enclose a set of spatial points availably, whose characteristics were suitable to solve the missing problem of 3D surface scanning and to make effective estimation of the area of missing regions. Combining 3D scanning constraints mainly based on limited dimensions in Euclidean space [11,12] and the visibility cone concept which was simply described as scanning vector visual area [13,14], the sampling points and directions of scanning were determined, so that the specific scanning path was planned through computed points and directions. To implement this improvement scanning method, it required the assistance of an automatic platform in order to execute the operations, so that a robotic manipulator mounted with a handy 3D scanner was designed and applied, since its movement trajectories were accurate and the performances of scanning paths were also guaranteed.

2. Rough scanning

The general topography and contour information of object surface were quickly obtained by rough scanning. Through determining the information collected by 3D scanner and analysing the point cloud data of boundaries, it was able to provide necessary computational data support to path planning in specific scanning. From the perspective of discretization, transforming the 3D information of measured surface into point cloud data, the missing scanned regions were determined by the discretization algorithm [9]. As depicted in Figure 1, the original point cloud data was divided into several layers based on the values along Z axis and the data of each layer was projected onto the XOY plane. According to the accuracy of 3D scanner, the distance threshold of projected point cloud was defined by T. It also defined that adjacent projection points on the projection plane were $P_i(x_i, y_i)$ and $P_{i+1}(x_{i+1}, y_{i+1})$ respectively. If the Euclidean norm from P_i to P_{i+1} satisfied the equation (1), it was determined that there was a missing region between P_i and P_{i+1}, that was, 3D information was missing in this region. Meanwhile, P_i and P_{i+1} represented the boundary points of the missing region.

$$\left\| P_i - P_{i+1} \right\| = L_i > T \tag{1}$$

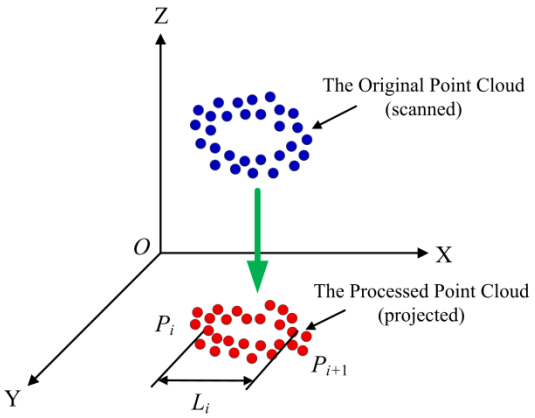

Figure 1. The missing regions determined by point cloud data.

There also existed invalid scanning region which contained incomplete data in surface gridding process, reading and processing the 3D information of the triangular patches included in the region,

the estimated value of the normal direction of missing region $\boldsymbol{N}_m$ was expressed by the average value of the normal directions of triangular facets $\boldsymbol{N}_j$ as

$$\boldsymbol{N}_m = \frac{\sum_{j=1}^{m} \boldsymbol{N}_j}{\left|\sum_{j=1}^{m} \boldsymbol{N}_j\right|} \qquad j = 1, 2, \cdots, m \tag{2}$$

3. Specific scanning

In the specific scanning process, firstly sampling points of scanning was arranged in order to confirm the repair scanning centre and then scanning paths were planned

3.1 Sampling point arrangement

The MEB theory and the shrinkage optimization algorithm were introduced to enclosing compute the boundary point cloud of the missing regions. The MEB of missing region B_r was obtained with the centre $C_0(x_0, y_0, z_0)$ and the radius R_0 as depicted in Figure 2(a). The ball centre C_0 was also treated as the geometric centre of missing region. Since the estimated value of the normal direction of missing region was $\boldsymbol{N}_m$, the plane Π was defined through the ball centre C_0 and perpendicular to the normal direction $\boldsymbol{N}_m$, so that the sampling points should be on plane Π. Defining arbitrary point $C(x, y, z)$ on plane Π, then $C_0C(x\text{-}x_0, y\text{-}y_0, z\text{-}z_0)$, the plane Π was expressed by equation (3).

$$\boldsymbol{N}_m \bullet \boldsymbol{C}_0\boldsymbol{C} = \boldsymbol{0} \tag{3}$$

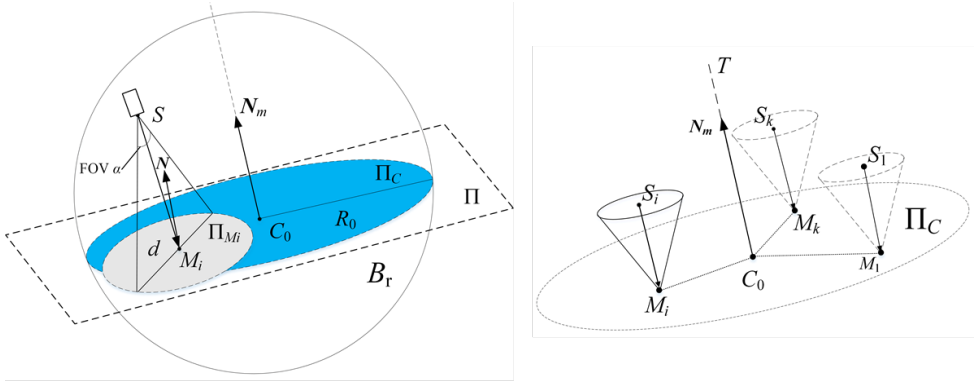

(a) (b)

Figure 2. Specific scanning planning based on MEB.

The cross section of the plane Π and the MEB B_r was the circle Π_C with the centre C_0 and radius R_0, as depicted in Figure 2(a) in blue. Making the sampling point M_i of missing region being on the axis of the field of vision (FOV), the intersection of the set of FOVs corresponding to the viewpoint S and the plane Π formed the circle of vision (COV) Π_{Mi} with the centre M_i and the diameter d, as depicted in Figure 2(a) in grey. To ensure that all positions of missing regions of 3D surface were collected, the problem was converted to compute the minimum number of COVs Π_{Mi} required to cover the circle Π_C. Considering that the missing region was usually small, so that the difference between the radius of the circle Π_{Mi} and the radius of the circle Π_C was little, therefore, the minimum number of FOVs required to cover the MEB's cross section was computed by circumference division method and the spatial coordinates of the sampling points were arranged. Taking the diameter d of COV Π_{Mi} as the chord length of circle Π_C to equally divide the circumference of the circle Π_C, defining that φ was the central angle corresponding to the string d and x was the number of required strings, the relationship between x and φ was expressed by $x=[2\pi/\varphi+1]$, where [.] represented to be rounded down.

According to the circumference division method, the number of strings x depends on the relationship between d and R_0. When $x>5$, the missing region was relatively larger, which rarely appeared, so only

the situation when x<5 was considered. When x=1, the sampling point M_i was the centre of the circle Π_C, when x=3 or x=4, the number of sampling points was equal to the number of strings, and the sampling point M_i was located at the midpoint of each chord of equally divided circumference. Since the missing region was quite small in most cases, it was usually required to arrange one sampling point.

3.2 Scanning path planning

On the theoretical basis of the 3D scanning constraints and the visibility cone concept, the scanning viewpoints were arranged and the scanning directions were confirmed, as depicted in Figure 2(b). In order to ensure that each position of the missing region was collected, the viewpoints S_i were arranged on the axis parallel to the normal direction N_m through the sampling point M_i. The height of the viewpoint S_i from the sampling point M_i was between the near depth and the far depth of scanning vision and the scanning direction was C_0N_m. In specific scanning process, path planning was actually to determine the order of each scanning viewpoint, and then to confirm the corresponding movement trajectory of the scanner through the spatial position of each viewpoint. The procedure of scan path planning was described as following:

- To determine the order of scanning viewpoints: connecting each viewpoint in the clockwise direction and scanning the viewpoint on the axis C_0T in the end.
- To plan the scanning path of adjacent viewpoints: applying the cubic spline interpolation method [15] to plan the trajectories between the two adjacent S_{i-1} and S_i so as to ensure the stability of the whole scanning process.
- To confirm the movement trajectory of scanner: establishing the relative spatial position relationship between the object and the scanner, transforming the planned path of viewpoints into the real trajectory of scanner, to complete the 3D scanning and surface reconstruction.

4. Robot based scanning system

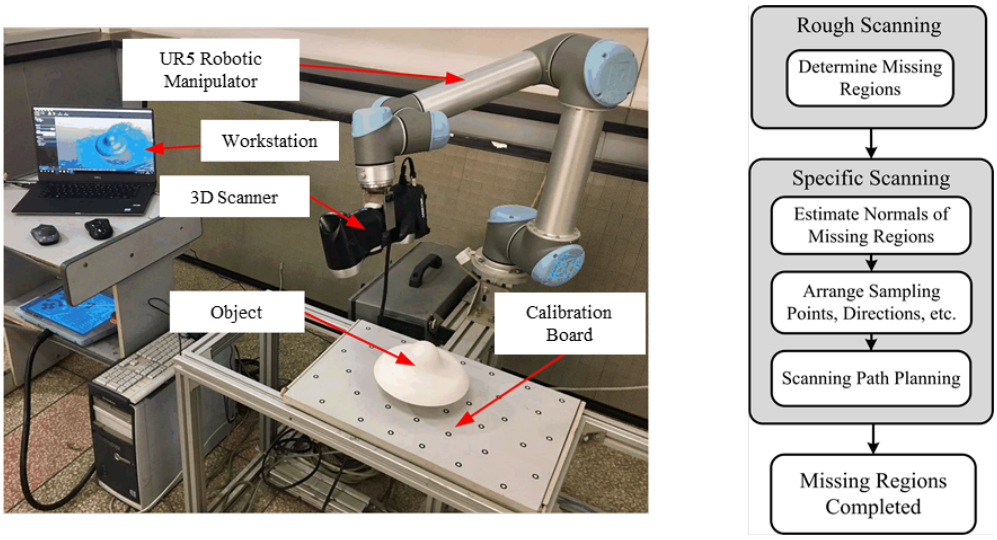

(a) (b)

Figure 3. Design and workflow of robot based scanning system.

In order to verify the effects of the two-stage scanning method, an experimental scanning system was set up as depicted in Figure 3(a). It consisted of a HandyScan300 3D scanner, a UR5 robotic manipulator, a Dell graphics processing station, a calibration board and other components. The main parameters of 3D scanner: the vision distance of was 300mm, the depth of field was 250mm, and the coverage area was 225mm x 250mm at the vision height. Since UR5 robot has six degrees of freedom,

strong load capacity and wide work range, it was applied with a customized gripper mounted on the end to carry the 3D scanner in the scanning process. The workflow of this robot based scanning system of the whole robot was depicted in Figure 3(b), and it was also applied with the two-stage scanning method.

In the rough scanning, it required that to scan the surface of object at a faster speed to obtain the general point cloud data, which was able to increase the scanning efficiency with no need for high requirements of 3D information integrity. Similar to the motions of rough machining, the robot carried the scanner to perform alternating movements. In the process, the boresight axis of scanner was always vertically down, the scanning route interval was set to 150mm, and the speed of scanning was set to 0.3m/s, which was faster than the scanning speed by holding the scanner with hands. To roughly scan the object depicted in Figure 3(a), after processing 3D information collected by the scanner, relevant point cloud data was obtained, in which the total number of points was 1.31657E+5 and the superficial area after fitting was 3.858923E+4mm^2. It was easily determined that the missing regions are M1 and M2 based on initial scanning results as depicted in Figure 4(a).

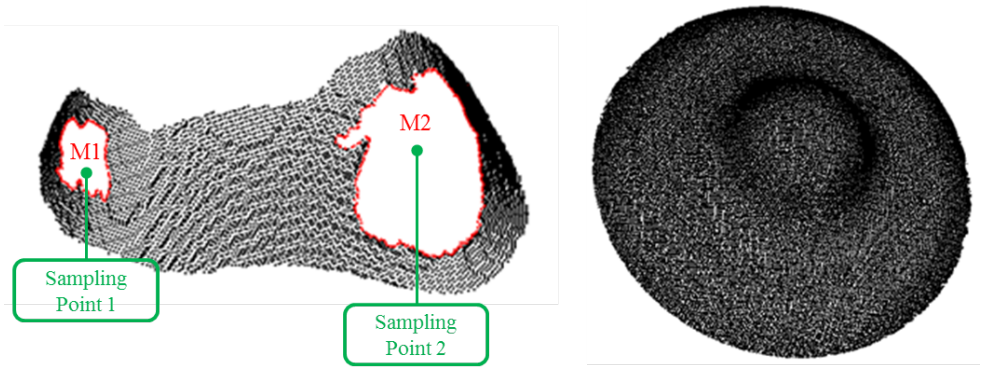

Figure 4. The process of 3D surface scanning.

Applying the shrinkage optimization method to enclosing compute the point cloud of boundaries of missing regions M1 and M2 respectively, the MEB centre of M1 was obtained at (72.86, -226.61, 188.22) and the radius was 8.12mm, similarly the MEB centre of M2 was at (23.35, -236.77, 198.62) and the radius was 16.07mm. Considering the geometric relationships in vision distance, depth of field, coverage area and other parameters of scanner, the radius of COV was computed to be 93.75mm. The radiuses of circles produced from the MEBs of M1 and M2 intersecting with respective Π planes were 8.12mm and 16.07mm respectively, and the ratios to the radius of COV were 0.09 and 0.17 respectively. The number of sampling points was set to 1 by the circumference division method. Therefore, the sampling points were arranged and the scanning viewpoints, the scanning directions and the scanning paths were all able to be planned.

Then transforming the scan path into the movement trajectories of robot, guided the robot equipped with 3D scanner was guided to repair scanning the missing regions through specific sampling points and scanning directions, the complete point cloud data of object as depicted in Figure 4(b). After that, the number of points included in scanned point cloud data of object became 1.34053E+5 and superficial area after fitting became 3.93980E+4mm^2, increased by 2396 and 808.77mm^2 respectively, compared to the obtained data in rough scanning, which meant that the quality of scanning was improved and the topography of object surface was completed in the end.

5. Conclusion

In order to pursuit the quality of scanning in a faster speed, a new two-stage method was presented in 3D laser surface scanning process for unknown object. In the first rough scanning, the general contour

and topography of surface were obtained as point cloud data, and the missing regions were determined by using chord length method. In the second specific scanning, focusing on the missing regions, the exact sampling locations and the scanning paths were planned by MEB theory and regional coverage theory. The improvement method was implemented in a robot based scanning system which contained a robotic manipulator and a handy scanner, with the advantages of convenient operability and fast movability. Utilizing a robotic platform, it not only enhanced the stability of scanning, but also reduced the errors caused by shock and vibration in the scanner's movements. Finally, relevant experiments were carried out and the results were evaluated for the feasibility and effectiveness of this two-stage scanning method, and both of speed and quality of scanning were improved.

6. Acknowledgments

The authors would like to acknowledge that this study was partly supported by National Natural Science Foundation of China (Grant No. 61603067) and Liaoning Province Natural Science Foundation (Grant No. 2015020068).

7. References

[1] Li Y F, He B and Bao P 2005 *Sensors and Actuators A: Physical* **22** 335-44
[2] Kriegel S, Rink C, Bodenmüller T, Narr A, Suppa M and Hirzinger G 2012 *Int. Conf. on Intelligent Robots and Systems* (Vilamoura, Portugal) 2850-56
[3] Lu K Q, Wang W and Chen Z C 2010 *J. Mechanical Engineering* **46** 143-49
[4] Wu Q, Zou W and Xu D 2016 *Int. J. Automation and Computing* **13** 42-52
[5] Cervantes J, Li X, Yu W and Li K 2008 *Neurocomputing* **71** 611-19
[6] Liang Y D, Sun J F, He F B and Lu Y H 2015 *China Mechanical Engineering* **26** 756-61
[7] He F B, Liang Y D, Sun J F, Wang Z X and Guo C 2015 *J. Mechanical Engineering* **51** 64-70
[8] Song Q J, Xiao X M, Jiang H Y and Zhao X G 2015 *J. Mechanical Science and Technology* **29** 3467-73
[9] Wu B H and Wang S J 2004 *Mechanical Science and Technology* **23** 1363-65
[10] Zhou X L, He B W and Li Y F 2009 *Prod. Int. Conf. on Robotics and Biomimetics* (Guilin, China) p 965-70
[11] Kawasaki H and Furukawa R 2007 *Prod. 6th. Int. Conf. on 3-D Digital Imaging and Modeling* (Montreal, QC, Canada) p149-58
[12] Ozan Ş and Gümüştekin Ş 2014 *Digital Signal Processing* **24** 231-43
[13] Lee K H and Park H P 2000 *Robotics and Computer-Integrated Manufacturing* **16** 201-10.
[14] Lee R S, Lin Y H, Tseng M Y and Wu W S 2010 *Int. J. Computer Integrated Manufacturing* **23** 630-39
[15] Gasparetto A and Zanotto V 2010 *Advances in Engineering Software* **41** 548-56